PHYSICAL REVIEW C VOLUME 20, NUMBER 5 NOVEMBER 1979

Positive pion-nucleus elastic scattering at 40 MeV

M. Blecher, K. Gotow, D. Jenkins, and F. Milder*
Virginia Polytechnic Institute and State University, Blacksburg, Virginia 24061

F. E. Bertrand, T. P. Cleary, E. E. Gross, and C. A. Ludemann
Oak Ridge National Laboratory, Oak Ridge, Tennessee 37830

M. A. Moinester,† R. L. Burman, M. Hamm, R. P. Redwine,‡ and M. Yates-Williams
Los Alamos Scientific Laboratory, Los Alamos, New Mexico 87545

S. Dam, C. W. Darden III, R. D. Edge, D. J. Malbrough,§ T. Marks,‖ and B. M. Preedom
University of South Carolina, Columbia, South Carolina 29208

(Received 8 May 1979)

Differential cross sections for elastic scattering of 40 MeV positive pions from ^{12}C, ^{16}O, ^{40}Ca, ^{90}Zr, and ^{208}Pb were measured at 18 angles in the angular range 25°–160°. Relative uncertainties of 2.5% to 7% and overall normalization uncertainties of 4% to 7% were obtained. An optical potential fit of the data indicates that while the magnitudes of the strength parameters, except for $\mathrm{Re}b_1$, are different from values obtained from free πN scattering amplitudes, the variation of these magnitudes with target mass is roughly as predicted by the impulse approximation. Coulomb effects, especially in the cases of ^{90}Zr and ^{208}Pb, are extremely important, but impossible to unambiguously separate from the strong interaction in the optical model.

[NUCLEAR REACTIONS Elastic scattering of 40 MeV π^+ from ^{12}C, ^{16}O, ^{40}Ca, ^{90}Zr, ^{208}Pb. Angular distributions: $25° < \theta_L < 160°$. Optical model and partial-wave analysis of cross-section data.]

INTRODUCTION

The subject of pion-nucleus elastic scattering has received much attention over the past decade. The elastic scattering process was expected to be sensitive to nuclear structure effects which could not be studied as easily with other probes. An understanding of elastic scattering is necessary before more complex processes like inelastic scattering, charge exchange, and double charge exchange can be interpreted. However, data taken in the energy region of the (3, 3) pion-nucleon (πN) resonance are relatively insensitive to details of the nuclear interior. The angular distributions are reasonably well fit with first order zero-range optical potentials of the Kisslinger type with the potential strength parameters derived from free πN scattering amplitudes.[1-3]

For energies well below the (3, 3) πN resonance the πN cross section is small and thus the nucleus is considerably more transparent to pions. Here the elastic scattering process is expected to be sensitive to the nuclear interior.[4] In previous publications[5,6] angular distributions for π^+ ^{16}O (40 and 50 MeV) and π^+ ^{12}C (50 MeV) elastic scattering were presented. As in earlier work[7,8] it was found that a Kisslinger type potential would fit the data if the potential strength parameters (which were independently varied to obtain best fits) had values quite different from the values derived from free πN scattering amplitudes. Other recent experiments in the low energy domain confirm this conclusion.[9-11]

In addition, the analyses[5,6] of the π^+ ^{16}O and π^+ ^{12}C data indicated that the angular distributions were unrealistically sensitive to the nuclear radius. Such sensitivity implies that a Kisslinger type optical potential does not provide a completely adequate description of the elastic scattering process. One analysis[12] of the 50 MeV π^+ ^{16}O data has demonstrated the importance of the higher order Lorentz-Lorenz effect. Other theories[13,14] which include all first order effects, i.e., no fixed scatterer approximation, inclusion of binding and Pauli effects, correct πN versus π-nucleus kinematics, and also include the second order effect of true pion absorption phenomenologically, provide a reasonable reproduction of the data. It is important to note that each of the effects mentioned above makes a significant contribution to the calculated cross sections.[15] In this paper the elastic differential cross sections obtained at 40 MeV for π^+ scattering from ^{12}C, ^{16}O, ^{40}Ca, ^{90}Zr, and ^{208}Pb are presented along with optical potential and partial wave fits of the data.

EXPERIMENTAL DETAILS

The experiment was performed on the low energy pion beam line at LAMPF. The major features of the experimental method have been described elsewhere.[5] In this section a brief description of the method used to obtain the 40 MeV data is reported.

The targets were mounted on plastic frames and oriented at 40° to the pion beam [intensity ~5×10^6 π^+/sec, spot size ~2 cm(horizontal)×1 cm(vertical)]. Identical target frames, without targets, were used for background measurements. Table I lists the characteristics of each target. The specific targets chosen have closed shells and form the core nuclei for many mass regions of interest in nuclear reactions. Transitions to the lowest excited states are easily separated from the elastic scattering with plastic scintillation detectors. Such a detector system[16] is capable of an energy resolution for 40 MeV π^+ of about 1 MeV. Our overall resolution was somewhat larger depending upon target thickness. The CH_2 target was used to obtain elastic scattering cross sections from hydrogen in order to provide an independent check of the absolute normalization.

Plastic scintillator detector telescopes in a multidetector array were used for the measurements.[5] Two angle sets, each consisting of ten angles, were used to span the angular range from 25°–160° at a total of eighteen different angles. Since ten angles were measured simultaneously, the shapes of the angular distributions are well determined. Two detectors, one in transmission geometry at 100° and one in reflection geometry at 90° remained fixed, and served to check the normalization between angle sets.

At very forward and backward angles (25°–45° and 150°–160°) the high rate of decay muons from the beam necessitated an additional requirement of observing the $\pi\rightarrow\mu\nu$ decay before accepting an event.[17] The efficiencies of the telescopes requiring this signature were measured by matching the yields obtained at angles of 90°, 100°, and 105° with the $\pi\rightarrow\mu\nu$ telescopes to the yields measured by telescopes without the $\pi\rightarrow\mu\nu$ identification.

In order to determine the incident pion flux the in-beam and $(\pi^+, 2p)$ monitors previously described[5] were used. Briefly, the in-beam monitor was used at low beam intensity to determine directly the number of pions in the beam and thus calibrate the $(\pi^+, 2p)$ monitor. The latter monitor, sensitive to $(\pi^+, 2p)$ reactions in the target, was used to obtain the number of pions on target at high intensities. Additional monitoring was provided by two small scintillators, mounted at an angle well inside the Jacobian cusp angle, which counted decay muons from the beam.[18] This monitor was calibrated using the $(\pi^+, 2p)$ monitor. It has a distinct advantage over the $(\pi^+, 2p)$ monitor in that it can also be used for empty target runs. Finally, as mentioned above, the elastic scattering of π^+ from protons was measured in the same manner. These cross sections were compared with the best available data[19] and with current phase shift analyses[20] in order to check the normalization. It should be emphasized that the measured π^+p cross sections were not used to provide the overall normalization.

In order to extract cross sections from the raw data the following effects must be considered: (a) pion decay between target and detector and between target and in-beam monitor, (b) pion reactions and elastic scattering in the detector, (c) multiple scattering and finite beam geometry, (d) finite detector acceptance of 4°. The last effect is particularly important at forward angles where the cross sections vary rapidly with angle. A full discussion of the magnitudes of these effects can be found elsewhere.[5]

TABLE I. Target characteristics.

Target	Construction	Isotopic enrichment (%)	Dimensions (cm×cm)	Mass per unit area (g/cm^2)
^{12}C	graphite sheet		14 ×14	0.223
CH_2	polyethylene sheet		14 ×14	0.251
H_2O	gelled with 1.5% gelatin mixture		10.8 ×10.8	0.390
^{40}Ca	sheet	96.94	5.08× 5.08	0.203
^{90}Zr	foil	97.6	5.08× 5.08	0.120
^{208}Pb	foil	98.7	6.35× 6.35	0.154

TABLE II. Elastic π^+-nucleus differential cross sections. The energies quoted are the π^+ laboratory kinetic energy at the center of the target. The normalization errors δN are quoted in percent. The relative errors are quoted in mb/sr. δN was obtained by adding in quadrature the average systematic error for the nucleus in question with the error in the target thickness and pion flux (typically ±3.3%).

	^{12}C, 40.0 MeV		^{16}O, 40.0 MeV		^{40}Ca, 40.2 MeV		^{90}Zr, 40.4 MeV		^{208}Pb, 40.4 MeV	
θ_L (deg)	$\theta_{c.m.}$ (deg)	$\frac{d\sigma}{d\Omega_{c.m.}}\left(\frac{mb}{sr}\right)$	$\theta_{c.m.}$ (deg)	$\frac{d\sigma}{d\Omega_{c.m.}}\left(\frac{mb}{sr}\right)$	$\theta_{c.m.}$ (deg)	$\frac{d\sigma}{d\Omega_{c.m.}}\left(\frac{mb}{sr}\right)$	$\theta_{c.m.}$ (deg)	$\frac{d\sigma}{d\Omega_{c.m.}}\left(\frac{mb}{sr}\right)$	$\theta_{c.m.}$ (deg)	$\frac{d\sigma}{d\Omega_{c.m.}}\left(\frac{mb}{sr}\right)$
25	25.4	7.97 ± 1.19	25.3	19.10 ± 2.16	25.1	75.6 ± 5.90	25.1	417 ± 25	25	2180 ± 155
30			30.3	10.79 ± 0.68	30.1	42.8 ± 2.70	30.1	223 ± 12	30	937 ± 50
40	40.6	4.16 ± 0.20	40.4	6.09 ± 0.31	40.2	22.7 ± 0.90	40.1	91.8 ± 3.2	40	318 ± 12
45	45.7	3.32 ± 0.14	45.5	5.33 ± 0.29	45.2	19.8 ± 0.80	45.1	78.0 ± 2.8	45	198 ± 7.3
55	55.8	2.63 ± 0.10	55.6	4.37 ± 0.22	55.2	14.5 ± 0.50	55.1	38.6 ± 1.0	55	50.9 ± 1.9
60	60.8	2.43 ± 0.09			60.2	12.7 ± 0.40	60.1	31.1 ± 0.90	60.1	35.8 ± 1.3
70	70.9	2.69 ± 0.10	70.7	4.67 ± 0.08	70.3	12.0 ± 0.40	70.1	20.0 ± 0.70	70.1	13.9 ± 0.60
80	80.9	3.28 ± 0.11	80.7	6.14 ± 0.13	80.3	12.5 ± 0.40	80.1	14.4 ± 0.50	80.1	8.36 ± 0.52
85	85.9	4.04 ± 0.13	85.7	6.79 ± 0.11	85.3	12.5 ± 0.40	85.1	11.6 ± 0.40	85.1	8.23 ± 0.50
90	90.9	4.36 ± 0.13	90.7	7.29 ± 0.09	90.3	10.9 ± 0.40	90.1	9.42 ± 0.40	90.1	8.62 ± 0.52
100	100.9	5.72 ± 0.17	100.7	8.82 ± 0.10	100.3	11.1 ± 0.40	100.1	8.45 ± 0.42	100.1	12.5 ± 0.60
105	105.9	6.09 ± 0.16	105.7	8.80 ± 0.18	105.3	8.36 ± 0.28	105.1	8.33 ± 0.41	105.1	15.1 ± 0.70
110	110.9	6.42 ± 0.19	110.7	8.82 ± 0.15	110.3	7.60 ± 0.27	110.1	8.41 ± 0.39	110.1	15.1 ± 0.70
120	120.8	6.72 ± 0.18	120.6	9.21 ± 0.16	120.3	6.62 ± 0.26	120.1	10.1 ± 0.50	120.1	17.2 ± 0.70
130	130.7	6.75 ± 0.17	130.5	8.26 ± 0.16	130.3	6.30 ± 0.27	130.1	12.4 ± 0.40	130	16.5 ± 0.70
140	140.6	6.93 ± 0.17	140.4	8.14 ± 0.16	140.2	5.27 ± 0.24	140.1	14.9 ± 0.50	140	17.1 ± 0.80
150	150.5	7.33 ± 0.31	150.4	6.77 ± 0.17	150.1	5.61 ± 0.84	150.1	17.2 ± 0.90	150	17.8 ± 1.20
160	160.3	7.32 ± 0.30	160.2	6.39 ± 0.17	160.1	5.84 ± 0.88	160.0	19.7 ± 1.20	160	18.3 ± 1.70
	δN = ±4%		δN = ±7%		δN = ±4%		δN = ±7%		δN = ±6%	

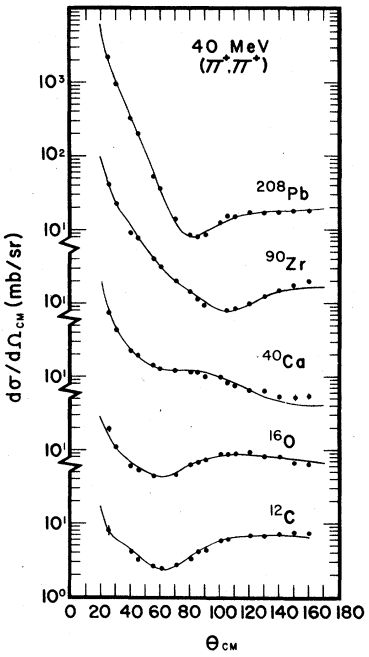

FIG. 1. Angular distributions at 40 MeV of positive pions on ^{12}C, ^{16}O, ^{40}Ca, ^{90}Zr, ^{208}Pb. The solid curves are optical-model fits to the data.

EXPERIMENTAL RESULTS

The differential cross sections are listed in Table II. The errors quoted in mb/sr are the relative errors, determined by statistics, and uncertainties in efficiencies, solid angles, etc. A minimum relative error of 2.5% is assumed regardless of counting statistics. Differences, between the cross sections measured by counters fixed at the same angle for both angle sets give an indication of the magnitude of the systematic errors. The average differences were: for ^{12}C 2%; for ^{16}O 2%; for ^{40}Ca 2%; for ^{90}Zr 6%; for ^{208}Pb 3.5%. The normalization error quoted in percent is obtained by adding in quadrature the systematic errors, the errors in target thickness, and the error in the pion flux. The energy listed is the pion laboratory energy at the center of the target.

To illustrate the trend of the data as a function of mass number the differential cross sections are plotted in Fig. 1. For the light nuclei the shapes of the angular distributions exhibit a minimum at about 65°, which is similar to effects seen at 50 MeV.[5-9] This minimum has been interpreted as resulting from the interference between s and p wave πN amplitudes.[21] For backward angles the ^{12}C cross sections remain fairly constant, whereas for ^{16}O there is a gradual decrease. The ^{12}C cross sections obtained from targets of ^{12}C and CH_2 agree within the overall normalization uncertainties, again indicating the consistency of the data. The ^{12}C cross sections are in excellent agreement with those measured at 38.6 MeV at TRIUMF.[11]

The minimum in the cross sections observed at ~65° for the light nuclei gradually disappears as the mass number of the target increases and the Rutherford cross section assumes greater importance. Only a suggestion of a minimum is apparent in the case of ^{40}Ca. In the mass region $A \gtrsim 40$ a different minimum in the cross section is observed to move to more forward angles as the nuclear mass increases, which is characteristic of a diffraction minimum.

The present measured $\pi^+ p$ angular distributions, taken as a check of the overall normalization, are plotted in Fig. 2 along with those obtained by Bertin *et al.*[19] In addition, the cross sections predicted by phase shift analyses[20] using data below 100 MeV (excepting the present data) are also plotted. Again the errors shown on our data points are relative errors only (the overall normalization error is ±~4%). Except at small angles and one extreme backward angle the agreement between the two data sets is good. At small angles the present data are in better agreement with the phase shift predictions, even though the latter were influenced by the Bertin *et al.*[19] data. However, in view of the discrepancies between the data sets and between data and phase shift predictions, one can see the importance of making an independent absolute normalization measurement for low energy pion-nucleus scattering experiments.

ANALYSES AND RESULTS

The present data analysis has the limited objective of discovering general trends as a function of mass. Partial wave analysis is a convenient parametrization of angular distribution data. However, in this case, it is not easy to associate the results of a partial wave analysis with the πN interaction or nuclear structure. Optical model calculations are more restrictive than a partial wave analysis as a particular model for the off-shell πN t matrix and nuclear structure are included.

The form of the πN t matrix used to calculate the optical potential[12] is

$$t(E(k), \vec{q}, \vec{q}') \propto \sum_{i=0}^{1} \frac{b_i(E)(\vec{q}\cdot\vec{q}')^i (k^2+\alpha_i^2)^2}{(q^2+\alpha_i^2)(q'^2+\alpha_i^2)}, \quad (1)$$

where k and E are the on-shell pion momentum and energy, $\vec{q}$ and $\vec{q}'$ are the off-shell initial and final pion momenta (they serve as integration variables in going from t matrix to cross section), b_0 and b_1 are the complex S and P wave strengths, and α_0 and α_1 are parameters related to the πN

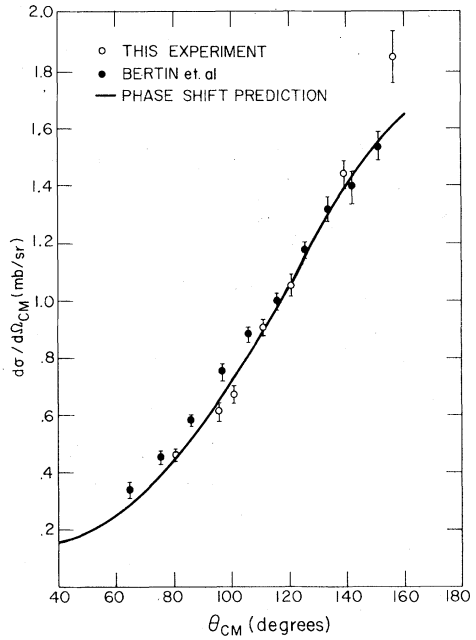

FIG. 2. Angular distributions of $\pi^+ + p$ at 40 MeV.

interaction range ($\alpha_0 = \alpha_1 = \infty$ gives the Kisslinger model). Values of α_1 range from 300 MeV/c to 700 MeV/c[10] and in this range the 40 MeV cross sections are rather insensitive to the exact value of α_i. In this analysis $\alpha_0 = \alpha_1 = 500$ MeV/c has been used.

The nuclear density was taken to have a Woods-Saxon form:

$$\rho(r) = \rho_0 [1 + \exp((r - c)/a)]^{-1}, \quad (2)$$

where c is the half-density radius, a is the diffuseness, and ρ_0 is the normalization factor. The values of c and a can be obtained from electron scattering data as described elsewhere.[10] The values used in this analysis were: ^{12}C, $c = 2.45$ fm, $a = 0.35$ fm; ^{16}O, $c = 2.7$ fm, $a = 0.41$ fm; ^{40}Ca, $c = 3.68$ fm, $a = 0.58$ fm; ^{90}Zr, $c = 4.86$ fm, $a = 0.57$ fm; ^{208}Pb, $c = 6.50$ fm, $a = 0.54$ fm.

The search code[22] varies the strength parameters b_0 and b_1 to minimize χ^2 between the calculated differential cross sections and the data. The values of b_0 and b_1 which give the best fit to the data plus the resulting χ^2 values are listed in Table III, and the calculated cross sections are plotted with the data in Fig. 1. Even though $\mathrm{Im}b_0 < 0$ (and thus pion producing) for ^{16}O, ^{40}Ca, and ^{208}Pb, the overall potential is unitary as the inelasticity of each partial wave is less than unity. Also listed in Table III are the parameters b_0 and b_1 as derived from free πN scattering data using an impulse approximation.[8,23] Though the magnitudes of the fitted and derived strengths are different, except for $\mathrm{Re}b_1$, the trends as a function of mass are similar:

(i) $\mathrm{Im}b_0$ and $\mathrm{Im}b_1$ show essentially no variation with mass,

(ii) $\mathrm{Re}b_0$ and $\mathrm{Re}b_1$ are slightly increasing and decreasing with mass, respectively. This is qualitatively consistent with the effect of neutron excess in ^{90}Zr and ^{208}Pb.

Also listed in Table III are the real parts of the forward strong scattering amplitude and the total cross sections (derived from the imaginary part of the forward strong scattering amplitude) as calculated from the optical potential. It has been pointed out[24] that in a model dependent calculation of this kind it is not possible to separate unambiguously Coulomb and strong effects completely. The total cross section listed does not correspond to the cross section for removal of pions from the incident beam via the strong interaction. Further, when Coulomb effects become very important, as in the case of ^{208}Pb, the low value of the calculated cross section is expected. The sign change in the

TABLE III. 40 MeV π^+-nucleus elastic scattering optical model parameters. The total cross sections and real parts of the forward strong scattering amplitude for π^+ and π^0 are calculated with the listed parameters. The parameters predicted from πN scattering in the impulse approximation are listed.

Nucleus	$\mathrm{Re}b_0$ (fm^3)	$\mathrm{Im}b_0$ (fm^3)	$\mathrm{Re}b_1$ (fm^3)	$\mathrm{Im}b_1$ (fm^3)	χ^2/n_D	$\sigma^{\pi^+}_{\mathrm{total}}$ (mb)	$\mathrm{Re}f^{\pi^+}$ (0°)	$\sigma^{\pi^0}_{\mathrm{total}}$ (mb)	$\mathrm{Re}f^{\pi^0}$(0°)
^{12}C	−3.33	0.19	6.17	1.16	1.2	208	0.88	207	1.05
^{16}O	−3.60	−0.16	6.45	1.41	4.1	277	1.02	277	1.33
^{40}Ca	−3.04	−0.04	5.79	1.14	4.5	558	1.33	626	3.08
^{90}Zr	−2.82	0.02	6.42	1.22	5.0	1332	−0.75	2080	4.11
^{208}Pb	−1.36	−0.27	5.42	1.64	3.0	441	−6.08	3775	3.84
Free πN									
$Z = A/2$	−1.09	0.65	6.32	0.50					
^{90}Zr	−0.48	0.68	5.87	0.47					
^{208}Pb	0.08	0.69	5.45	0.45					

real part of the forward strong scattering amplitude for ^{90}Zr and ^{208}Pb is also due to Coulomb effects. These results can be understood by calculating the forward strong amplitude for π^0-nuclear scattering in the optical model with the same strength parameters as specified in Table III. This calculation is only approximately correct as the π^0 energy is taken equal to that of the π^+. The results of the calculation appear in Table III and indicate that $\sigma_{\text{total}}^{\pi^0}$ varies approximately linearly with A and that $\text{Re}f^{\pi^0}(0^\circ)$ does not change sign. Thus any conclusions concerning systematic trends in the strong amplitude can be made only after the Coulomb effects are understood.

A potential, once obtained, can be used to generate phase shifts δ_l and inelasticities η_l. The phase shift parameters generated from the optical potentials which best fit our data are listed in Table IV. Phase shift parameters were also obtained from a partial wave analysis using the following scattering amplitude[25]:

$$f(\theta) = f_c(\theta) + \frac{1}{2ik}\sum_{l=0}^{l_{\max}}(\eta_l e^{2i\delta_l} - 1) \times e^{2i\sigma_l}(2l+1)P_l(\cos\theta), \quad (3)$$

TABLE IV. 40 MeV π^+-nucleus elastic scattering partial wave (PW) parameters deduced from the optical potential and from a partial wave analysis.

Nucleus	l	η_l^{opt}	δ_l^{opt} (deg)	η_l^{PW}	δ_l^{PW} (deg)	χ_{PW}^2/n_D
^{12}C	0	0.92	−12.9	0.67	−15.9	0.82
	1	0.86	10.0	0.99	7.7	
	2	0.97	2.9	0.94	3.4	
	3	1.00	0.3			
^{16}O	0	0.97	−15.5	0.98	−17.3	2.52
	1	0.84	10.7	0.90	8.3	
	2	0.95	4.3	0.94	3.6	
	3	1.00	0.6			
^{40}Ca	0	0.85	−14.9	0.88	−12.5	1.74
	1	0.81	8.9	0.72	13.3	
	2	0.89	8.3	0.92	7.5	
	3	0.98	2.2	1.00	2.5	
	4	1.00	0.4	1.00	0.3	
^{90}Zr	0	0.79	−26.8			
	1	0.65	7.1			
	2	0.71	16.4			
	3	0.90	6.9			
	4	0.99	1.4			
	5	1.00	0.7			
^{208}Pb	0	0.86	1.1			
	1	0.72	11.8			
	2	0.65	18.7			
	3	0.79	10.8			
	4	0.94	3.2			
	5	0.99	0.6			

where f_c is the point Coulomb amplitude, $l_{\max}$ is the highest partial wave considered, η_l and δ_l represent the magnitude and phase of the strong scattering amplitude, and σ_l is the relativistic point Coulomb phase shift for the lth partial wave. The values of η_l and δ_l are varied to obtain best unitary fits to the data. Such an analysis is much less restricted than an optical model calculation and typically yields the best possible fits of the data. Such fits serve as checks on the smoothness of the data and indicate whether the errors have been estimated correctly. Reasonable fits to the data are obtained for a small number of partial waves. For ^{12}C and ^{16}O only one solution is found. These solutions are listed in Table IV and are seen to be very similar to the parameters found from the optical potential analysis. For the nuclei with $A \geq 40$ many partial wave solutions are possible. In the case of ^{40}Ca one of the possible solutions yields parameters similar to those found from the optical potential analysis, and they are listed in Table IV also. For ^{90}Zr and ^{208}Pb the Coulomb effects dominate the cross sections and the use of a point Coulomb amplitude in a partial wave analysis is suspect. The parameters obtained do not resemble those obtained from an optical model analysis.

SUMMARY

Data for the elastic scattering of 40 MeV positive pions on nuclei spanning the periodic table have been presented. An optical potential fit of the data indicates that while the magnitudes of the strength parameters, except for $\text{Re}b_1$, are different from values obtained from free πN scattering amplitudes, the variation of these magnitudes with target mass is roughly as predicted by the impulse approximation. Coulomb effects, especially in the cases of ^{90}Zr and ^{208}Pb, are extremely important, but impossible to unambiguously separate from the strong interaction in the optical model.

ACKNOWLEDGMENTS

The authors would like to thank the LAMPF staff for their support and encouragement. We extend special thanks to N. W. Hill of ORNL for his assistance in the design of electronics components for the "π-μ" systems. We also thank W. R. Gibbs, B. F. Gibson, and G. J. Stephenson, Jr. for providing us with their partial wave and optical model codes and for many helpful discussions. This work was supported in part by the National Science Foundation, by the U. S. Department of Energy, by the Office of Naval Research, and by the Union Carbide Corporation under contract with the U. S. Department of Energy.

*Present address: Spire Corporation, Bedford, Mass. 01730.
†On leave from Tel Aviv University, Ramat Aviv, Israel.
‡Present address: Physics Department and Laboratory for Nuclear Science, MIT, Cambridge, Mass. 02139.
§Present address: Louisiana State University, Baton Rouge, La. 70800.
||Present address: Los Alamos Scientific Laboratory, Los Alamos, N.M. 87545.

[1]F. Binon, P. Duteil, J. P. Garron, J. Görres, L. Hugon, J. P. Peigneux, C. Schmit, M. Spighel, and J. P. Stroot, Nucl. Phys. B17, 168 (1970); M. Blecher, K. Gotow, D. K. Anderson, R. Kerns, R. Minehart, K. Ziock, R. W. Bercaw, J. S. Vincent, and R. Johnson, Phys. Rev. C 10, 2247 (1974).

[2]E. Boschitz, in *Proceedings of the Seventh International Conference on High Energy Physics and Nuclear Structure, Zurich, Switzerland, 1977,* p. 133.

[3]B. Zeidman, C. Olmer, D. F. Geesaman, R. L. Boudrie, F. H. Seeinssen, J. F. Amann, C. L. Morris, H. A. Thiessen, G. R. Burleson, M. J. Devereux, R. E. Segel, and L. W. Swenson, Phys. Rev. Lett. 40, 1316 (1978).

[4]M. M. Sternheim and R. R. Silbar, Annu. Rev. Nucl. Sci. 24, 249 (1974).

[5]D. J. Malbrough, C. W. Darden, R. D. Edge, T. Marks, B. M. Preedom, F. E. Bertrand, T. P. Cleary, E. E. Gross, C. A. Ludemann, K. Gotow, R. L. Burman, M. A. Moinester, and R. P. Redwine, Phys. Rev. C 17, 1395 (1978).

[6]M. A. Moinester, R. L. Burman, R. P. Redwine, M. A. Yates-Williams, D. J. Malbrough, C. W. Darden, R. D. Edge, T. Marks, S. H. Dam, B. M. Preedom, F. E. Bertrand, T. P. Cleary, E. E. Gross, C. A. Ludemann, M. Blecher, K. Gotow, D. Jenkins, and F. Milder, Phys. Rev. C 18, 2678 (1978).

[7]J. F. Marshall, M. E. Nordberg, Jr., and R. L. Burman, Phys. Rev. C 1, 1685 (1970).

[8]E. H. Auerbach, D. M. Fleming, and M. M. Sternheim, Phys. Rev. 162, 1683 (1967).

[9]J. F. Amann, P. D. Barnes, M. Doss, S. A. Dytman, R. A. Eisenstein, and A. C. Thompson, Phys. Rev. Lett. 35, 426 (1976); S. A. Dytman, J. F. Amann, P. D. Barnes, J. N. Craig, K. G. R. Doss, R. A. Eisenstein, J. D. Sherman, W. R. Wharton, R. J. Peterson, G. R. Burleson, S. L. Verbeck, and H. A. Thiessen, Phys. Rev. Lett. 38, 1059 (1977).

[10]H. Dollard, K. L. Erdman, R. R. Johnson, H. R. Johnston, T. Masterson, and P. Walden, Phys. Lett. 63B, 416 (1976).

[11]R. R. Johnson, T. G. Masterson, K. L. Erdman, A. W. Thomas, and R. H. Landau, Nucl. Phys. A296, 444 (1978).

[12]W. R. Gibbs, B. F. Gibson, and G. J. Stephenson, Jr., Phys. Rev. Lett. 39, 1316 (1977).

[13]L. C. Liu and C. M. Shakin, Phys. Rev. C 16, 333 (1977).

[14]R. H. Landau and A. W. Thomas, Nucl. Phys. A302, 461 (1978).

[15]B. M. Preedom, in *Proceedings of the Seventh International Conference on High Energy Physics and Nuclear Structure, Zurich, Switzerland, 1977,* p. 119.

[16]M. J. Saltmarsh, B. M. Preedom, R. D. Edge, and C. W. Darden, III, Nucl. Instrum. Methods 105, 311 (1972).

[17]D. Axen, G. Duesdieker, L. Felawka, C. H. Q. Ingram, G. Jones, M. Salomon, and W. Westlund, Nucl. Instrum. Methods 118, 435 (1974).

[18]E. A. Wadlinger, Nucl. Instrum. Methods 134, 243 (1976).

[19]P. Y. Bertin *et al.*, Nucl. Phys. B106, 341 (1976).

[20]R. Arndt, L. D. Roper, and V. Zidell, to be published.

[21]H. Thies, Phys. Lett. 63B, 43 (1976).

[22]W. R. Gibbs, B. F. Gibson, G. J. Stephenson, Jr., private communication.

[23]G. Rowe, M. Salomon, and R. H. Landau, Phys. Rev. C 18, 584 (1978).

[24]M. D. Cooper and M. G. Johnson, Nucl. Phys. A260, 352 (1976).

[25]W. R. Gibbs, B. F. Gibson, C. J. Stephenson, Jr., Los Alamos Scientific Laboratory Report No. LA-UR-77-1404 (unpublished).